AGU PUBLICATIONS

Water Resources Research

RESEARCH ARTICLE
10.1002/2016WR019041

Special Section:
Emergent Aquatic Carbon-Nutrient Dynamics as Products of Hydrological, Biogeochemical, and Ecological Interactions

Benthic biofilm controls on fine particle dynamics in streams

K. R. Roche [1], J. D. Drummond [2], F. Boano [3], A. I. Packman [1], T. J. Battin[4], and W. R. Hunter[5]

[1]Department of Civil and Environmental Engineering, Northwestern University, Evanston, Illinois, USA, [2]Integrative Freshwater Ecology Group, Centre for Advanced Studies of Blanes (CEAB-CSIC), Blanes, Girona, Spain, [3]Department of Environment, Land and Infrastructure Engineering, Politecnico di Torino, Italy, [4]Stream Biofilm and Ecosystem Research Laboratory, School of Architecture, Civil and Environmental Engineering, École Polytechnique Fédérale de Lausanne, Lausanne, Switzerland, [5]Queen's University Marine Laboratory, School of Biological Sciences, The Queen's University of Belfast, Northern Ireland

Abstract Benthic (streambed) biofilms metabolize a substantial fraction of particulate organic matter and nutrient inputs to streams. These microbial communities comprise a significant proportion of overall biomass in headwater streams, and they present a primary control on the transformation and export of labile organic carbon. Biofilm growth has been linked to enhanced fine particle deposition and retention, a feedback that confers a distinct advantage for the acquisition and utilization of energy sources. We quantified the influence of biofilm structure on fine particle deposition and resuspension in experimental stream mesocosms. Biofilms were grown in identical 3 m recirculating flumes over periods of 18–47 days to obtain a range of biofilm characteristics. Fluorescent, 8 μm particles were introduced to each flume, and their concentrations in the water column were monitored over a 30 min period. We measured particle concentrations using a flow cytometer and mesoscale (10 μm to 1 cm) biofilm structure using optical coherence tomography. Particle deposition-resuspension dynamics were determined by fitting results to a stochastic mobile-immobile model, which showed that retention timescales for particles within the biofilm-covered streambeds followed a power-law residence time distribution. Particle retention times increased with biofilm areal coverage, biofilm roughness, and mean biofilm height. Our findings suggest that biofilm structural parameters are key predictors of particle retention in streams and rivers.

Key Points:
- We quantified biofilm-particle interactions by fitting a stochastic mobile-immobile model to observations from laboratory flume experiments
- Fine particle retention was positively correlated with biofilm height, roughness, and streambed coverage
- Results can be integrated within the stochastic mobile-immobile framework to assess the effects of biofilms on fine particle dynamics

Supporting Information:
- Supporting Information S1

Correspondence to:
K. R. Roche,
k-roche@u.northwestern.edu;
W. R. Hunter,
w.hunter@qub.ac.uk

Citation:
Roche, K. R., J. D. Drummond, F. Boano, A. I. Packman, T. J. Battin, and W. R. Hunter (2017), Benthic biofilm controls on fine particle dynamics in streams, *Water Resour. Res.*, *53*, 222–236, doi:10.1002/2016WR019041.

Received 9 APR 2016
Accepted 5 DEC 2016
Accepted article online 17 DEC 2016
Published online 11 JAN 2017

1. Introduction

The streambed is a highly reactive habitat of stream ecosystems. Here, biogeochemical transformations are largely driven by sediment-attached and matrix-enclosed microbial communities, called biofilms [*Jones and Mulholland*, 1999; *Fellows et al.*, 2006; *Battin et al.*, 2008; *Battin et al.*, 2016]. Biofilms control critical ecosystem processes, provide entry for organic carbon into the stream food web, and influence the amount and lability of carbon exported downstream [*Battin et al.*, 2008; *Tank et al.*, 2010; *Battin et al.*, 2016]. Abiotic features of streams (e.g., flow, streambed topography) are traditionally used to parameterize in-stream transport models, while biofilms are generally assumed to control only the transformation of reactive constituents (e.g., organic carbon and nutrients). However, there is growing experimental evidence that shows benthic biofilms modify water flow [*Nikora*, 2010; *Marion et al.*, 2014] and nutrient retention [*Battin et al.*, 2003; *Bottacin-Busolin et al.*, 2009; *Aubeneau et al.*, 2016] close to the streambed. This feedback may have implications for carbon fluxes in stream networks, since reactions largely occur at the sediment-water interface [*Jones and Mulholland*, 1999; *McClain et al.*, 2003; *Boano et al.*, 2014]. Biofilm-transport interactions are, therefore, critical but missing components of upscaled reactive transport models in streams.

Fine particulate organic matter (FPOM, $<$10 μm) are important sources of energy in streams and rivers [*Richardson et al.*, 2013]. Such particles derive from leaf litter and woody debris and from dissolved organic matter (DOM) that is adsorbed to soil and mineral particles. In streams, extracellular enzymes expressed by microbial heterotrophs in biofilms hydrolyze FPOM into its dissolved constituents, which then can be taken up and metabolized [*Richardson et al.*, 2013]. Factors such as enzyme concentration, particle size, and the degree of organo-mineral complexation can reduce reaction efficiency [*Dimock and Morgenroth*, 2006; *Hunter et al.*, 2016]. FPOM can be remobilized before they are completely degraded, illustrating the

dependence of FPOM metabolism on particle delivery and retention at the streambed and its biofilms [*Battin et al*., 2003; *Allan and Castillo*, 2007].

Particles deposit and resuspend episodically as they move through streams [*Cushing et al*., 1993; *Newbold et al*., 2005; *Harvey et al*., 2012; *Boano et al*., 2014; *Drummond et al*., 2014a]. In a well-mixed stream, particle deposition can be described by a first-order removal rate, which is generally reported as a deposition velocity, v_{dep} [*McNair and Newbold*, 2012]. This velocity typically exceeds the gravitational settling velocity predicted by Stokes' Law for small ($<$160 μm) particles [*Thomas et al*., 2001]. Particle resuspension is governed by a number of processes, resulting in a wide distribution of particle retention times. Turbulent eddies resuspend particles on the order of seconds by generating intermittent shear stresses at the streambed [*Ninto and Garcia*, 1996; *Niño et al*., 2003; *Soldati and Marchioli*, 2009]. Long-term retention (hours to months) is attributed to a combination of biological trapping and deeper sequestration within the stream sediments [*Newbold et al*., 2005; *Arnon et al*., 2010; *Harvey et al*., 2012; *Drummond et al*., 2014b].

Fluvial transport models have evolved to accommodate the wide range of particle residence times in streambeds. *Drummond et al*. [2014a] extended a continuous time random walk model, developed for solutes [*Boano et al*., 2007], and showed that particle residence time distributions (RTDs) follow a power law in streambeds. This mobile-immobile model conceptualizes particle transport as a series of discrete displacements and waits, which are stochastically represented as displacement-length and wait-time probability distributions. Because it assumes no prespecified RTD, the mobile-immobile model allows for parameterization of particle transport with distributions based on physical, independently verifiable processes. This allows deposition and resuspension to be parsed more explicitly than prior models, which have either lumped the two processes or parameterized exchange as an idealized transfer of mass between the stream and well-mixed storage zones [*Cushing et al*., 1993; *Paul and Hall*, 2002; *Newbold et al*., 2005]. Separation of deposition and resuspension dynamics is a crucial step to improving particle transport models, since these two processes are governed by different mechanisms [*Boano et al*., 2014; *Aubeneau et al*., 2015]. In situ observations of deposition and resuspension events remains an experimental challenge. Consequently, particle deposition and resuspension parameters are typically estimated from fits to in-stream particle concentrations and constrained by physical process models or independent observations, such as particle retention in sediments [*Drummond et al*., 2014a, 2014b].

Biofilms can substantially alter local environmental conditions on and within the streambed [*Battin et al*., 2016]. The biofilm extracellular polysaccharide matrix is a sticky substance that increases particle trapping, potentially retaining particles until the microbial community is remobilized by dispersal or scour [*Lock and Williams*, 1981; *Sutherland*, 2001; *Boulêtreau et al*., 2006; *Vignaga et al*., 2013; *Marion et al*., 2014]. Biofilms can also contain long, filamentous structures called streamers that extend into the turbulent boundary layer [*Stoodley et al*., 1999; *Besemer et al*., 2009], and their oscillations interact with the external flow field [*Taherzadeh et al*., 2012]. Mature biofilms are porous systems with highly variable topography [*Stoodley et al*., 2002; *Battin et al*., 2003]. These contributions to highly heterogeneous biofilm structure modify streambed roughness, which modulates turbulence intensity and solute transport near the streambed [*Larned et al*., 2004; *Nikora*, 2010; *Larned et al*., 2011]. In turn, the modified flow field is expected to enhance particle deposition, since particle settling is more likely in a region of low turbulence [*Bouwer*, 1987; *Drury et al*., 1993b; *Battin et al*., 2003].

Flow-biofilm interactions are expected to occur predominantly at vertical scales between 100 μm and 10 cm [*Nikora et al*., 1998, 2002; *Larned et al*., 2004, 2011], which coincides with the scales of biofilm structural heterogeneity [*Morgenroth and Milferstedt*, 2009]. Nonetheless, few experiments have analyzed the influence of biofilm structure on fine particle dynamics across this range of scales, limiting our understanding of which mechanisms control this biophysical feedback. In this study, we simultaneously quantified the mesoscale (10 μm to 1 cm) physical structure of benthic biofilms and suspended tracer particle concentrations in stream mesocosms. We fit the measured particle concentrations to a stochastic mobile-immobile model, allowing us to assess the influence of biofilm structure on particle deposition and resuspension dynamics. We hypothesized that benthic biofilms, differing in physical structure and overall streambed coverage, would differentially affect the deposition rate and resuspension probability of fine particles.

2. Materials and Methods

2.1. Mesocosm Setup

The study consisted of 12 individual experiments. For each experiment, we constructed a recirculating flume with a 300 cm L × 5 cm W × 12 cm H test section. The flume was gravity fed by a 1 L header tank and flowed into a 1 L effluent tank. We used an Eheim compact 1000 aquarium pump (Eheim GmbH & Co. KH, Deizisau, Germany), located at the bottom of the effluent tank, to recirculate water to the header tank. The two tanks were connected with 1.25 cm diameter vinyl tubing. The flume slope was adjusted to achieve a uniform water column depth across the entire test section (slope = 0.005). We lined the test section with 5 cm L × 5 cm W × 1 cm H ceramic tiles, which were acid washed and precombusted at 450°C for 8 h to remove organic matter. The flume setup is shown in Figure 1, and photographs are provided in supporting information.

Each experiment consisted of a biofilm growth period, followed by a 30 min period where we injected tracer particles and monitored their concentration in the water column. For the duration of the experiment, we recirculated water from an oligotrophic alpine lake (Lunzer See, Austria). The biofilm growth period ranged from 0 to 47 days across experiments, which allowed for the development of biofilms with a range of structural properties. During the growth period we replaced flume water every second day to ensure adequate carbon and nutrients were available for microbial growth. We replaced water by first draining a small volume of water from the effluent tank. We then added an equivalent volume of replacement water to the effluent tank. These steps were repeated until one flume volume (approximately 3 L) was added. Flumes were located indoors and operated under 12 h light:dark cycles. A benthic biofilm formed on the tiles during this period.

2.2. Flume Hydrodynamics

At the end of the growth period we measured stream depth and flow rate. Flow rate was measured by diverting the return flow to a 1 L graduated cylinder and measuring filling time. We calculated mean flume velocity $U = Q/dw$, where U is the mean flume velocity (cm/s), Q is the flow rate (cm^3/s), d is the water column depth (cm), and w is the flume width (cm). Stream Reynolds number is reported as $Re = 4UR_h/\nu$, where ν is the kinematic viscosity of water (cm^2/s). The Froude number is defined as $Fr = U/\sqrt{gd}$, where g is the gravitational constant (9.81 m^2/s). Shear velocity, u^* (cm/s), was calculated using the Colebrook-White equation for free-surface flow (see supporting information).

2.3. Fine Particle Release and Monitoring

We immediately released a pulse of fine fluorescent tracer particles (EcoTrace, ETS Worldwide Ltd., Helensburgh Scotland) at the end of the growth period. Tracer particles were stained with rhodamine dye. Mean particle diameter was 8.4 ± 7.0 μm and mean particle volume was 25.4 ± 18.6 μm^3 as measured on an EyeTech particle size (Ankersmid, Eindhoven, Netherlands), and their specific gravity was 2.65. Estimated particle settling velocity was 0.044 mm/s, calculated from Stokes' Law. Particles were suspended in 50 mL of a 1 g/L sodium tetraborate solution (dissolved in deionized water) to prevent aggregation. This yielded a slug with 12.4 g/L particle concentration. We agitated this suspension for 30 s and immediately injected it into

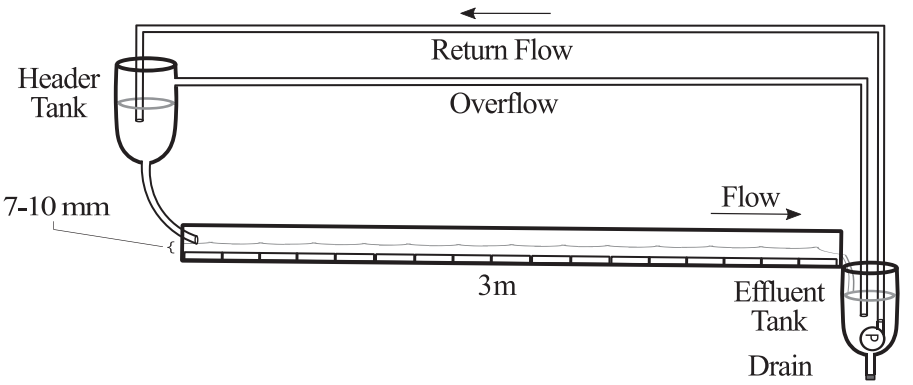

Figure 1. Mesocosm setup.

the flume header tank (Figure 1). We then monitored particle concentrations in the water column for 30 min following injection. During this time, we collected water column samples using standard 2 mL tubes inserted into the water column at the flume outlet (before flume water mixed with effluent tank water). We initially collected samples at 5 s intervals and gradually decreased the sample rate over the course of the 30 min monitoring period (5 s intervals from 0 to 2 min; 1 min/2–5 min; 5 min/5–30 min). Samples were immediately refrigerated until particle analysis.

We quantified particle concentrations with a Cell Lab Quanta flow cytometer (Beckman Coulter Inc., Brea, CA, USA). Briefly, water samples were mixed for 60 s using a vortex mixer. Five hundred microliters of sample water was then drawn into the flow cytometer's flow cell at a rate of rate of 60 μL min^{-1} for between 2 and 5 min (automated duration based on concentration). Particle concentrations were quantified by measuring fluorescence in the green and orange spectra using the Cell Lab Quanta SC software package. Concentrations were normalized against background autofluorescence of the flume water and verified against detection limits of the instrument, following procedures described in *Drummond et al*. [2014a, 2014b]. We smoothed each concentration time series using a standard moving-window averaging function in Matlab (R2015b, Mathworks Inc., USA), as described in supporting information.

Along with the particles, we coinjected a NaCl solution (50 mL, 100 mS/cm) as a conservative tracer, which we measured as electrical conductivity in the flume effluent tank (WTW Cond 3210, Xylem Inc., Weilheim, Germany). This solute pulse was detectible for 3–4 flume recirculations before fully mixing with the water column. We determined flume recirculation time, t_r, defined as the mean time between successive peaks of the recirculating solute pulse, and the volume of recirculating water in the flume, V_f, via the observed dilution of the solute tracer under well-mixed conditions.

2.4. Biofilm Physical Structure

At the conclusion of the 30 min particle release and monitoring period, we stopped the flow and randomly removed three tiles located at least 15 cm (three tiles) from the flume inlet and outlet sections. Tiles were carefully transferred to petri dishes. Dishes were slowly filled with deionized water until the tile surface was submerged below 1–2 mm of water. We imaged three random but nonoverlapping locations on each tile, resulting in 9 (1 cm × 1 cm) scan areas for each experiment. The biofilm-covered tiles were imaged with a spectral-domain optical coherence tomography (OCT) microscope (Ganymede, ThorLabs, Newton, NJ, USA), which measures scattered and back-reflected light from an illuminated volume of the sample [*Huang et al*., 1991; *Xi et al*., 2006; *Wagner et al*., 2010]. The microscope records 2-D image slices in the x-z plane (10 μm pixels) at 10 μm intervals in the transverse (y) direction. Note that the particles were smaller than the pixel size and thus could not be resolved individually. Output files were TIFF stacks of 2-D greyscale images in the x-z plane. These files were postprocessed using Fiji (ImageJ platform 1.47h) [*Schindelin et al*., 2012; *Schneider et al*., 2012] and Matlab (R2015b). We manually straightened each image to assure biofilms were consistently measured from the base of the tile. We cropped the image stacks to minimize variability in light intensity, resulting in an average usable scan area of 3.8 cm^2 per experiment. Lastly, we binarized each image to distinguish biofilms from the water column. A full description of the postprocessing procedure is provided in supporting information.

We calculated several biofilm structural parameters from the OCT data to evaluate their influence on particle deposition and resuspension. Mean height measures the average overall height above the tile. We define roughness as the mean magnitude of variations in biofilm height, $|\overline{H-\overline{H}}|$. Areal coverage is defined as the fraction of tile surface area occupied by biofilm at least 10 μm thick, which is the smallest length scale we could resolve. For this calculation, we assume a unit spacing in the transverse (y) direction equal to the distance between scans (10 μm). All image analysis was performed using 2-D images, and 3-D composite images are provided for illustrative purposes only.

2.5. Stochastic Model for Fine Particle Deposition/Resuspension in Biofilms

We adapted the mobile-immobile model for particle transport in streams [*Boano et al*., 2007; *Drummond et al*., 2014a] to quantify fine particle dynamics in the recirculating flumes. The model assumes a partitioning of particles between a mobile and an immobile domain, considered to represent the water column and the streambed, respectively. Particle deposition events are mathematically represented as a transfer of particles from the mobile to the immobile domain, while particle resuspension is considered a transfer from the

immobile domain to the mobile domain. Particle concentrations are assumed to be spatially uniform in the water column.

A full model derivation is provided in supporting information. In brief, the concentration $C(t)$ of particles in a well-mixed water column is described by the following mass balance:

$$\frac{dC(t)}{dt}V_f = -N_{dep}(t)+N_{res}(t) \quad (1)$$

where V_f is the volume of water in the recirculating flume and $N_{dep}(t)$ and $N_{res}(t)$ denote the rate of particle deposition and resuspension, respectively (t^{-1}). $N_{dep}(t)$ is a first-order boundary flux to the streambed, governed by a rate constant, Λ (t^{-1}) [*Drummond et al*., 2014a]. Note that this rate is a depth-normalized deposition velocity, $\Lambda = v_{dep}/d$, where v_{dep} is the deposition velocity typically reported in field studies [*Thomas et al*., 2001; *Newbold et al*., 2005]. Following mobile-immobile stochastic theory [*Schumer et al*., 2003], we assume $N_{res}(t)$ depends on the number of particles in the immobile zone at time t, as well as on the time each particle has remained immobile since it deposited, $t-\tau$, where τ is the time of immobilization. These residence times are described by a probability distribution, $\varphi(t)$, which quantifies the probability a particle that has entered the immobile domain at time zero will return to the mobile domain at time t. Substitution of these expressions into equation (1) yields an integro-differential equation:

$$\frac{dC(t)}{dt} = \frac{\Lambda dA_b}{V_f}\left(-C(t)+\int_0^t C(\tau)\varphi(t-\tau)d\tau\right) \quad (2)$$

where Λ is the rate of particle immobilization (defined previously) and A_b is the area of the streambed. An algebraic solution for this expression can be derived after it is transformed to the Laplace domain ($\tilde{f}(u) = \int_0^\infty e^{-ut}f(t)dt$):

$$\tilde{C}(u) = \frac{C_0}{u+\frac{\Lambda dA_b}{V_f}(1-\tilde{\varphi}(u))} \quad (3)$$

where $\tilde{C}(u)$ is the Laplace-transformed concentration, C_0 is the initial particle concentration in the water column, u is the Laplace variable, and $\tilde{\varphi}(u)$ is the Laplace transformed resuspension time probability distribution. We assume $\varphi(t)$ takes the form of a power-law distribution ($\varphi(t) \sim t^{-(1+\beta)},\ 0<\beta<1$), where β is the power-law slope [*Berkowitz et al*., 2006]. Here decreasing values of β decrease the power-law slope, which increases the probability that a particle will be retained for very long times. The Laplace-transformed expression for $\varphi(t)$ was inserted into equation (3) to give the analytical solution for $\tilde{C}(u)$. This expression was inverse transformed to the time domain using a modified version of the CTRW MATLAB Toolbox (see supporting information [*de Hoog et al*., 1982; *Cortis and Berkowitz*, 2005; *Aubeneau et al*., 2015]), yielding a concentration time series for a fixed value of Λ and β. Note that this time series represents the Green's function solution, which represents the system response to a pulse of well-mixed particles entering the mobile domain at $t=0$. This solution can be convolved with a known source function (e.g., a constant or time-variable influx of particles) to predict a system response to more complex initial conditions.

This form of the mobile-immobile model requires a spatially uniform concentration in the water column, meaning particles are well mixed in all directions. For this reason, we only fit the model to concentrations measured after the injected pulse of particles was fully mixed with the flume water. We assume particles are fully mixed after the concentration peak is no longer detectable in the sample time series. The initial particle concentration, C_0, was determined by extrapolating the smoothed time series to time $t=0$. Particle concentrations can be treated as uniform in the vertical direction for very low values of the Rouse number ($p = v_g/\kappa u_*$, where p is the dimensionless Rouse number; v_g is the particle settling velocity; κ is Von Karman's coefficient, 0.4; and u_* is the shear velocity) [*Anderson and Anderson*, 2010]. To compare model outputs to experimental results, we normalize particle concentration by C_0 and normalize time by recirculation time, t_r.

We used the Maximum Likelihood Estimation method [*Montgomery and Runger*, 2010] to find values of Λ and β that best fit the concentration time series for each experiment. Details of the fitting procedure are

Table 1. Average Hydrodynamic Conditions Across All 14 Experiments

Slope	0.005
d (cm)	0.8 ± 0.1
Q (cm^3/s)	110 ± 13
U (cm/s)	25 ± 4
t_r (s)	25 ± 2
t_0 (s)	75 ± 27
Re	6300 ± 900
Fr	0.87 ± 0.20
Rouse no., p	$(6.8 \pm 1.3) \times 10^{-3}$
u^* (cm/s)	1.7 ± 0.3

presented in supporting information. All mobile-immobile modeling and MLE fitting steps were executed in Matlab (R2015b).

2.6. Correlations Between Model Parameters and Biofilm Structure

We used linear regression to quantify correlations between biofilm structural parameters and model fits for Λ and β across all experiments. Higher-order models were explored but did not substantially improve fits (results not shown). Model selection and validation were achieved by minimizing the Akaike Information Criterion (AIC) for each model [*Akaike*, 1974]. Statistical analysis was carried out in R [*R Development Core Team*, 2009].

3. Results

3.1. Flume Hydrodynamics

Average flow conditions are presented in Table 1. Flows did not vary considerably in time or between experiments. Stream depth varied by less than 1 mm across the entire flume test section for all experiments. The Rouse number was on the order of 10^{-3} to 10^{-2}, which supports our assumption of spatially uniform particle concentrations in the vertical direction [*Rouse*, 1939].

3.2. Biofilm Growth

OCT analysis revealed that biofilm growth started from individual microcolonies (day 18 of experiment) that coalesced through two-dimensional and three-dimensional proliferation. An extensive network of void spaces (pores) was visible in biofilms older than 30 days. Isolated streamers developed rather sparsely (1–3 per meter of streambed). Streamers were roughly 1 cm in length and extended through the depth of the water column (Figure 2e).

Results from all experiments are plotted in Figures 2a–2c, which show trends in structural parameters for biofilms of different ages. Mean biofilm height, biofilm roughness, and tile coverage increased rapidly between days 30 and 40. The streambed was nearly fully covered (80–99%) for biofilms older than 40 days. Mean biofilm height increased to a maximum between 140 and 160 μm, accounting for $\leq$ 2.5% of water column depth. Biofilm roughness reached a maximum of 86 μm by day 42.

3.3. Particle Dynamics and Model Fits

The pulse of particles mixed fully with the water column after 2–5 flume recirculations (0.8–2.3 min) in each experiment, indicated by the disappearance of the recirculating concentration peak (Figure 3). Water column concentrations then declined steadily throughout the remainder of the 30 min monitoring period for each experiment. Particle deposition was visible on the face of tiles. In experiments with no biofilm growth, we observed some trapping of particles under and between tiles. We found no particle accumulation below tiles in all other experiments, as the biofilms quickly covered the surface and clogged interstices between tiles.

Water column particle concentrations from each experiment were fit to the mobile-immobile model, as described in section 2. Example model fits are presented in Figure 4 for illustration. Best-fit parameter values for all experiments are provided in Table 2.

3.4. Correlation of Biofilm Structure and Mobile-Immobile Model Parameters

We found a negative correlation of biofilm age with the power-law slope of the resuspension RTD, β, demonstrating a significant increase in particle retention times for older communities ($R^2 = 0.58$, $p < 0.01$). Biofilm age did not influence deposition rate, Λ, ($R^2 = 0.02$, $p = 0.62$). Measured flow parameters did not correlate with Λ ($R^2 < 0.05$, $p > 0.50$ for all parameters in Table 1).

Linear regression results are provided in Table 3 for each biofilm structural parameter. All parameters were positively correlated with decreasing values of β, meaning they increased particle retention times. We chose

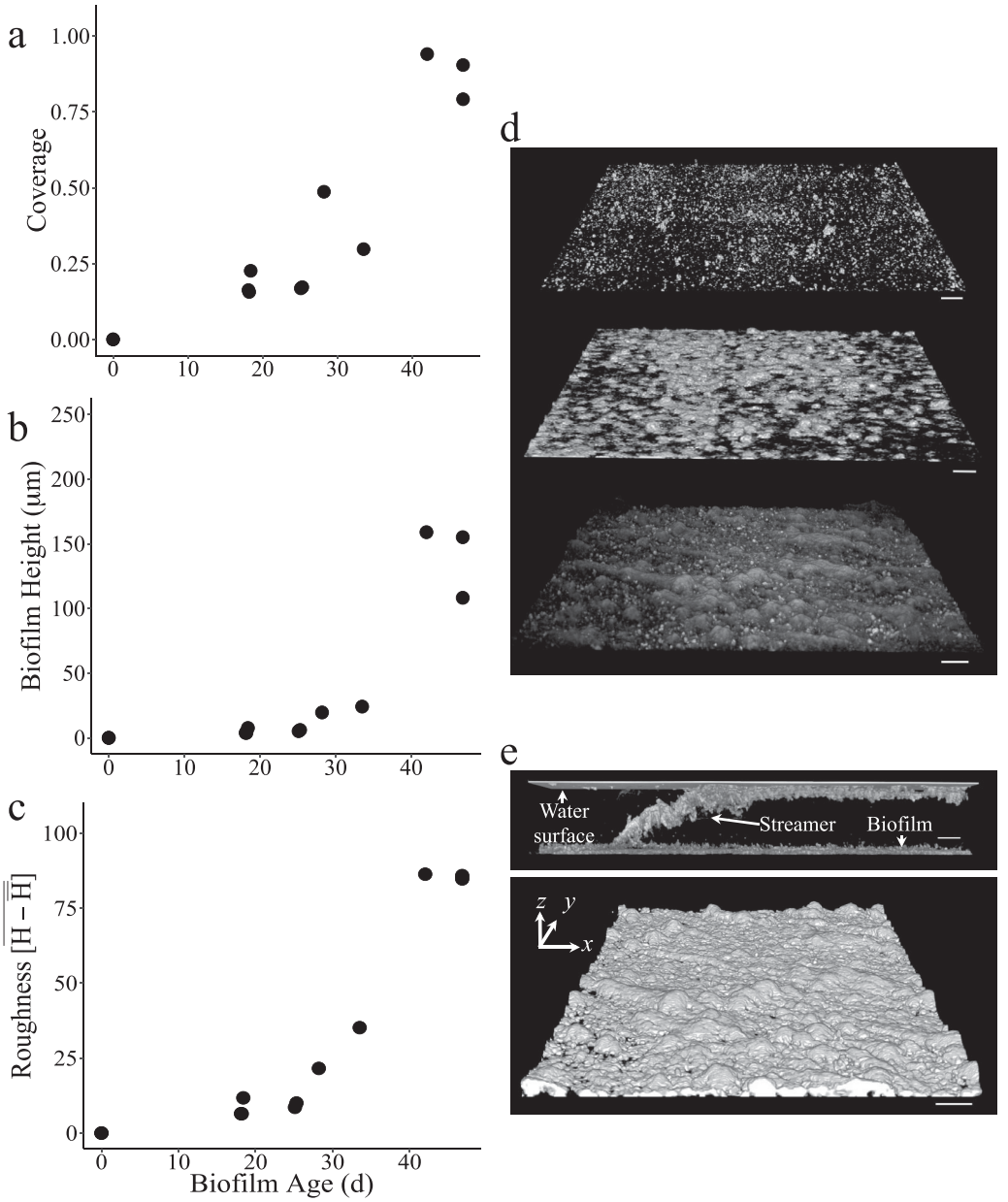

Figure 2. (a–c) Biofilm structural parameters measured from each experiment. (d) Processed OCT images for biofilms of different ages. Biofilm age (top-bottom) is 18, 28, and 42 days, respectively. Scale bars are 500 μm for all images. Initial biofilm microcolonies eventually coalesced into a continuous canopy, resulting in near 100% coverage. (e, top) Processed OCT images illustrating the three-dimensional structure of a streamer; the thin plane at the top of the image is a surface reflection from water in the sample container. (e, bottom) Surface topography of a 42 day biofilm. Basal dimensions for the image are 9 mm (along page) × 6.3 mm (into page). Mean biofilm height is 115 μm, and max height is 450 μm.

surface coverage as the most robust predictor of β for several reasons: (1) it provided the best goodness of fit and lowest AIC value, (2) coverage values spanned the entire range of possible values, and (3) data points were the least clustered for this parameter. The regression equation was (Figure 5):

$$\beta = 0.61 - 0.20 * Coverage \quad (R^2 = 0.49,\ p = 0.011) \tag{4}$$

Biofilm structure did not influence particle deposition rate in the flumes ($R^2 = 0.00$, $p \geq 0.92$). Values for Λ ranged between 0.16 and 0.88 s^{-1}. These rates equate to deposition velocities of 1.9–8.0 mm/s, which are

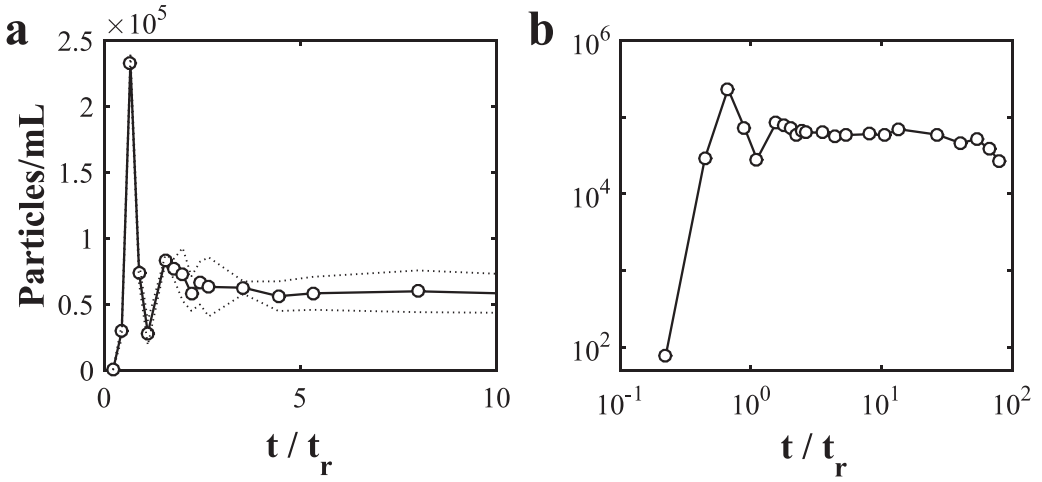

Figure 3. Particle concentrations following a pulse release for the experiment with 28 day biofilm. Biofilm is shown in the middle image of Figure 2d. Dotted lines show sample standard deviation for the measured particle concentrations. (a) Concentrations shortly after the pulse release (linear scale). (b) Concentrations over the entire deposition period (log scale).

40×–180× greater than the gravitational settling velocity (0.044 mm/s). Therefore, particle deposition was unaffected by settling. Although preferential deposition was observed behind isolated streamers, these structures only sparsely populated the flumes. Thus, they likely played a minor role in overall deposition.

We present cumulative residence time distributions to illustrate the relationship between β and particle retention (Figure 6). The plotted distributions are derived directly from model fits to β for each experiment (see supporting information), and they show the probability that a deposited particle will resuspend after a specified time, for a given value of β. We assume that resuspension probabilities are nonzero over a finite interval of times, with a minimum of $1/\Lambda_{max} \approx 1$ s, where Λ_{max} is the upper limit of the calculated values for Λ (0.88 s^{-1}). The maximum residence time is assumed to be 7 months, which corresponds to retention times observed for virus-sized particles in wetland mesocosms [*Flood and Ashbolt*, 2000]. The chosen values of β correspond to measured values at distinct periods of biofilm growth: a bare surface (0% coverage, β=0.72), an 18 day biofilm (23% coverage, β=0.57) and a 47 day biofilm (90% coverage, β=0.46). For low resuspension probabilities (<0.8), an increase in biofilm coverage results in a marginal increase in retention time (Figure 6a). This time difference grows substantially for resuspension probabilities approaching 1, which reflects the increased likelihood of very long retention times. For example, a

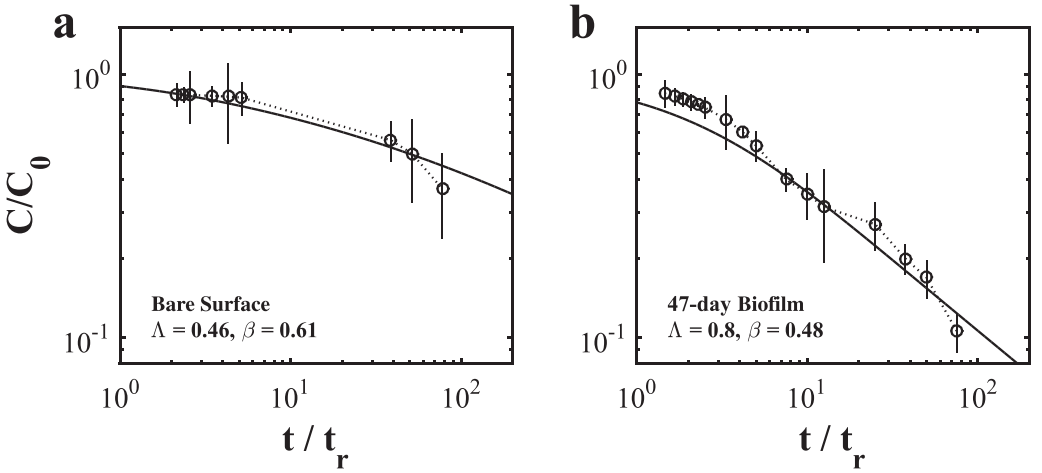

Figure 4. (a) Model fits of long-term particle concentrations for a streambed with no biofilm and (b) for a streambed with a 47 day biofilm. C_0 equals the initial particle concentration. t_r is the flume recirculation time. Data and error bars show the mean and standard deviation of triplicate concentration measurements, respectively.

Table 2. Measured Parameters and Mobile-Immobile Model Fits

Exp. No.	Days Growth	Coverage	Mean Height $\overline{H}$ (μm)	Roughness $\overline{H-H}$ (μm)	d (cm)	Q (cm^3/s)	U (cm/s)	Re	Fr	p ($\times 10^{-3}$)	Λ	β
1	0.0	0.00	0.01	0.0	0.70	116	33	7300	1.26	5.7	0.46	0.61
2	0.0	0.00	0.01	0.0	0.85	116	27	6900	0.95	6.2	0.26	0.72
3	18.1	0.16	3.88	6.5	0.80	109	27	6600	0.97	6.2	0.41	0.65
4	18.2	0.16	3.83	6.5	0.85	115	27	6800	0.93	6.3	0.46	0.44
5	18.4	0.23	7.61	11.8	0.80	112	28	6800	1.00	6.0	0.52	0.57
6	25.1	0.17	5.18	8.6	0.80	99	25	6000	0.88	6.7	0.88	0.60
7	25.3	0.17	6.07	10.0	0.85	101	24	6100	0.83	7.0	0.61	0.59
8	28.2	0.49	19.63	21.6	0.85	111	26	6600	0.90	6.4	0.16	0.49
9	33.5	0.30	24.17	35.2	0.95	75	16	4400	0.52	10.0	0.21	0.43
10	42.0	0.94	158.98	86.4	0.95	118	25	6800	0.81	6.4	0.23	0.42
11	46.8	0.79	108.29	85.9	0.10	88	18	5000	0.56	8.9	0.80	0.48
12	46.8	0.90	155.11	84.8	0.95	117	25	6800	0.81	6.4	0.49	0.46

particle will resuspend with 99.9% probability in 0.17 days for a bare surface versus 17 days for a bed with 90% coverage (Figure 6b).

4. Discussion

Reach-scale particle transport integrates multiple deposition and resuspension events. The relative frequencies of these events determine the balance of fine particle sequestration and export downstream. Thus, the different mechanisms that govern deposition and resuspension must be independently parameterized in fluvial transport models. Using a stochastic mobile-immobile model, we found that fine particle residence times on a biofilm-covered impermeable streambed followed a heavy-tailed power-law distribution (Figure 4). A similar result was found by *Drummond et al*. [2014a] for fine particles transported in natural streams, in which the authors attributed long-term particle retention to a combination of surface-subsurface (hyporheic) exchange, reversible filtration by sediments, and trapping by biofilms. Our results show that biofilm trapping alone results in a heavy-tailed power-law residence time distribution (RTD).

The power-law slope, β, correlated with mean biofilm height, roughness, and the fraction of the bed covered by biofilm (Table 3). Both physical trapping in biofilm pore spaces and electrostatic biofilm-particle interactions have been hypothesized to control particle interactions with the biofilm matrix. Early laboratory studies showed strong correlations between fine particle retention and biofilm thickness, suggesting that trapping within void spaces was most important [*Drury et al*., 1993a; *Okabe et al*., 1997]. However, particle trapping has also been observed in nascent (2 μm thick) biofilms that were too thin to contain pores large enough for particles [*Drury et al*., 1993b]. This finding and others have pointed to particle adhesion to biofilms as an alternative control on particle retention [*Xu et al*., 2005; *Morales et al*., 2007]. Biofilm extracellular polymeric substances are typically heterogeneous at the micrometer scale, allowing for varied steric and electrostatic interactions between the biofilm and particle surfaces that favor adhesion [*Bouwer*, 1987; *Sutherland*, 2001; *Searcy et al*., 2006; *Flemming and Wingender*, 2010].

The structural parameters reported in this study cannot be used to distinguish between physical trapping and particle adhesion to the biofilm, since we could not fully resolve pore structure across the thickness of mature biofilms or distinguish particles within the biofilm matrix. Nonetheless, we highlight the potential for biofilm surface coverage to be used as an integrated predictor of fine particle retention in streams and

Table 3. Linear Regression Results Between Model Parameters and Biofilm Structural Parameters[a]

Model Parameter	Structural Parameter	Effect	R^2	p-Value	d.f.	AIC
β	Coverage	+	0.49	0.01	10	−24.74
	Mean height, $\overline{H}$	+	0.36	0.04	10	−22.05
	Roughness, $H-\overline{H}$	+	0.45	0.02	10	−23.87
Λ	Coverage	N/A	0.00	0.92	10	
	Mean height, $\overline{H}$	N/A	0.00	0.96	10	
	Roughness, $H-\overline{H}$	N/A	0.00	0.92	10	

[a]A positive (+) effect indicates that increasing values of the structural parameter increased particle retention/deposition.

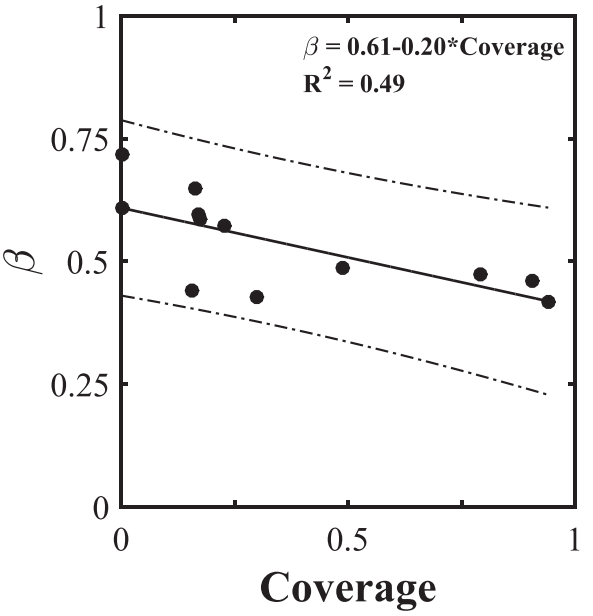

Figure 5. Linear regression fit showing relationship between power-law slope, β, and biofilm coverage. Solid line represents the best fit line (equation provided in plot), and dashed lines are 95% confidence intervals. Results for all parameters are reported in Table 3.

rivers, since it may be possible to estimate this parameter without the aid of sophisticated microscopic techniques (e.g., hand-held photography, surface inspection). Biofilm coverage may, therefore, be a suitable complement to other local observations that are used to parameterize solute and fine particle RTDs in upscaled, predictive stream models [*Boano et al*., 2007; *Stonedahl et al*., 2012; *Drummond et al*., 2014a; *Aubeneau et al*., 2015]. For example, *Drummond et al*. [2014a, 2014b] performed sediment column filtration experiments on 6 cm bed sediment cores to determine fine particle RTDs in hyporheic sediments of a lowland stream. They then used these results to parameterize a mobile-immobile model that accurately described particle transport and retention in a 221 m stream reach. This approach worked well because hyporheic filtration was the dominant control on particle deposition in the study reach. Biofilms are expected to increase fine particle retention both in the hyporheic zone and on the bed surface [*Thomas et al*., 2001; *Morales et al*., 2007; *Arnon et al*., 2010]. The results presented here provide a basis to include the effects of biofilm coverage and growth directly onto biofilm-covered portions of the streambed, as well as the effects of biofilm coatings of hyporheic sediments, on particle transport. Biofilm growth should then be considered as a secondary modification to the primary retention RTDs [*Margolin et al*., 2003], parameterized via experiments with biofilms grown on the relevant substratum or with in situ observations of particle retention in biofilms.

We found no significant correlation between biofilm structure and particle deposition rate, Λ, which was unexpected. Model fits for Λ were sensitive to concentrations at early times, which were highly variable. Estimates for Λ were, therefore, less robust than estimates for β, which were determined by concentrations

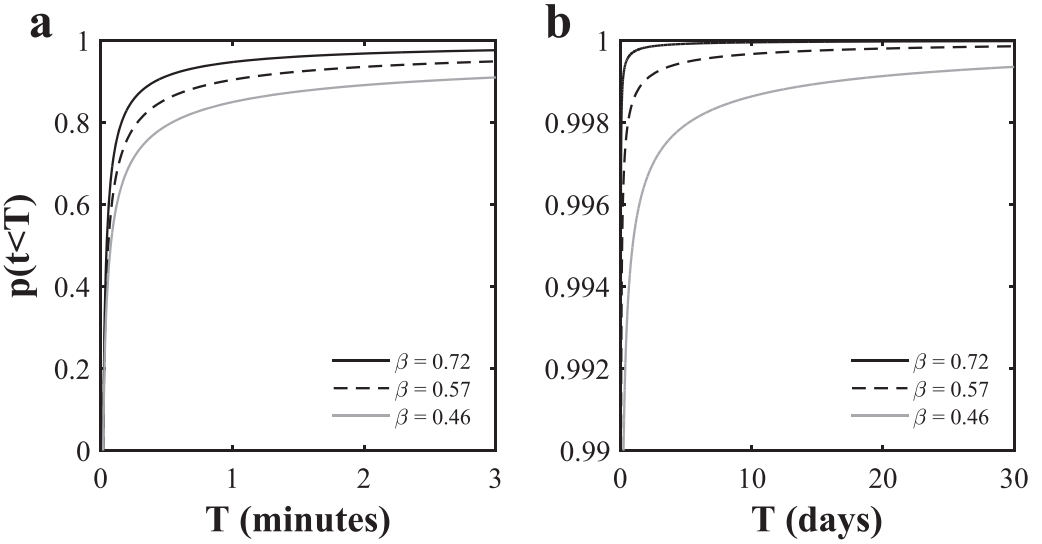

Figure 6. Cumulative resuspension time distributions for three measured values of power-law slope, β. A decrease in β increases the time required for a particle to reach a specific probability of resuspension. Distributions are similar at early times but differ substantially as resuspension probability approaches 1. (a) Distributions from 0 to 3 min. (b) Distributions from 0 to 30 d*ays*.

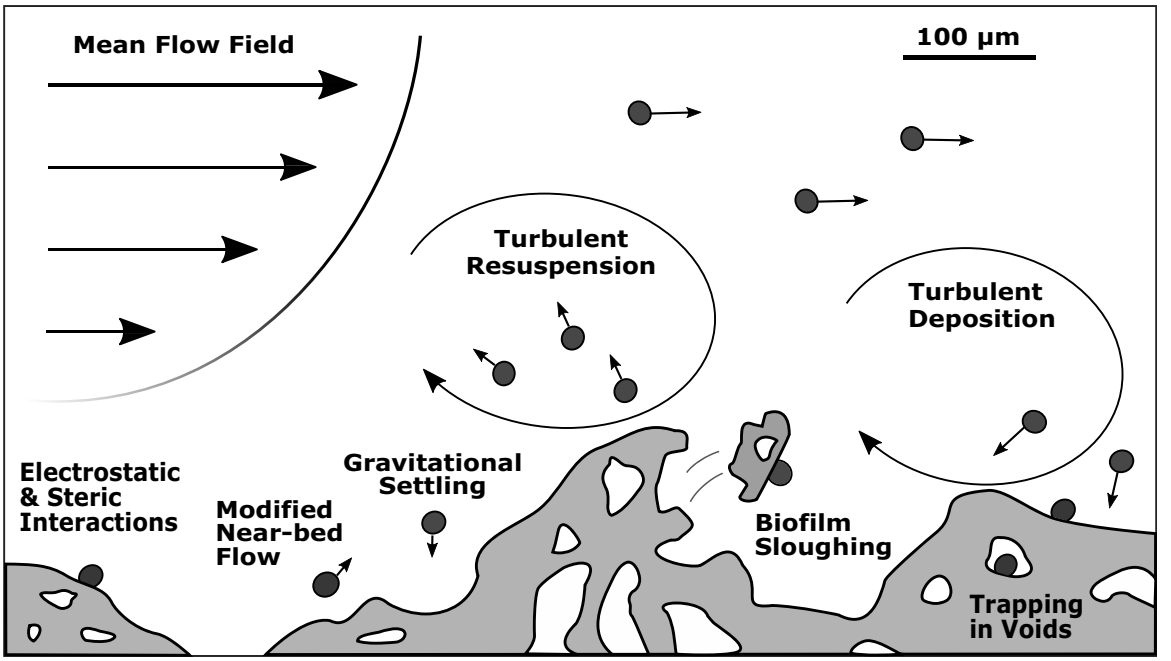

Figure 7. Conceptual diagram of mechanisms governing fine particle dynamics for a biofilm-covered streambed. Particle-biofilm interactions occur from scales ranging from biofilm pores (1 µm) to the depth of the stream (1 m).

at late times. Early-time removal depends on primary delivery and deposition of particles to the benthic biofilm. The influence of biofilm canopies on particle deposition merits further investigation, as biofilm structure is known to influence near-bed hydrodynamics (Figure 7). The flow field near the streambed is highly altered by biofilm patches, producing complex, three-dimensional flow patterns [*Costerton et al.*, 1995]. Particles are advected around and into the biofilm before colliding with the biofilm matrix [*Birjiniuk et al.*, 2014]. Positive correlations have been found between particle deposition and biofilm thickness [*Drury et al.*, 1993b], roughness [*Searcy et al.*, 2006; *DiCesare et al.*, 2012], and sinuosity [*Battin et al.*, 2003]. However, a definitive mechanistic understanding of structure-deposition interactions requires substantial technological improvements to simultaneously resolve biofilm pore structure, the three-dimensional flow structure around biofilms, and fine particle deposition and resuspension under turbulent conditions [*Weiss et al.*, 2013].

The correlation between biofilm coverage and β, quantified by equation (4), provides a functional relationship between the structure of streambed biofilms and RTDs for fine particles immobilized at the streambed. This relationship highlights one of the numerous process interactions between biofilm-covered streambeds and fine particles. Additional feedbacks recognized in engineered and natural systems are particle size relative to biofilm pore size [*Okabe et al.*, 1998; *Arnon et al.*, 2010], water chemistry [*Searcy et al.*, 2006; *Morales et al.*, 2007], biofilm modification of subsurface flowpaths [*Battin and Sengschmitt*, 1999; *Cuthbert et al.*, 2010; *Aubeneau et al.*, 2016], flow regime [*Okabe et al.*, 1997; *Okabe et al.*, 1998], and complex biofilm responses from interspecies interactions and environmental cues [*Battin et al.*, 2016; *Flemming et al.*, 2016]. Future research efforts should address the relative roles of these process interactions in controlling fine particle dynamics.

The small-scale feedbacks between biofilms and fine particles are a subset of the full range of feedbacks governing particle transport in streams. For example, the deposition dynamics modeled in the current study assume well-mixed particle concentrations in the water column, a condition that can vary over the meter scale in reaches with multiple geomorphological units (e.g., pool-riffle sequences). Particle fluxes are also coupled to terrestrial factors such as hillslope, vegetation type, and land use [*Gomi et al.*, 2002; *Tank et al.*, 2010], which can create kilometer-scale correlations with stream inputs. Fluxes are driven by high flow events, whose timing and intensity not only influence FPOM supply and retention [*Fisher and Likens*, 1973; *Newbold et al.*, 1997; *Harvey et al.*, 2012; *Karwan and Saiers*, 2012], but also control microbial community lifecycles by scouring and reconfiguring the streambed [*Power and Stewart*, 1987; *Biggs*, 1995; *Gomi et al.*, 2002]. However, as biofilms modify near-bed flows [*Nikora et al.*, 2002; *Larned et al.*, 2011] and stabilize sediments over their growth cycle, they create time-dependent feedbacks that can extend to these scales [*Vignaga et al.*, 2013].

Multiscale feedbacks present a challenge for the application of transport models to streams. Uniform, steady-state models can accommodate spatial and temporal variability if a sufficient separation of scales exists [*Nikora*, 2010; *Marion et al*., 2014]. Such models average over small-scale heterogeneities and are applied at scales much smaller than large geomorphic features or hydrologic events. Their validity thus depends on the intensity of feedbacks occurring across these scales. Our results contribute to a growing literature that suggests biofilm growth alters fine particle retention across a wide range of timescales [*Flood and Ashbolt*, 2000; *Thomas et al*., 2001; *Drummond et al*., 2014b]. These scales overlap with the timescales of hydrologic variability, which compromises the implicit assumption of stationarity in steady state transport models.

Scale interdependencies in fluvial ecosystems remain extremely difficult to characterize. Most experimental and field observations are restricted to a narrow range of spatial and temporal scales, which constrains our understanding of the predominant interactions beyond them. Future research efforts can address these limitations in three ways. First, the small-scale process interactions that control particle transport at the sediment-water interface must be properly characterized. New technologies will greatly improve our ability to directly observe these processes [*Weiss et al*., 2013]. Such direct observations are needed to independently estimate particle deposition and resuspension rates, which currently are inferred from water column observations. Second, future experimental and field studies must target process interactions over yet-unexplored scale ranges. For instance, our μm-to-cm scale observations of a biofilm-retention feedback must be tested at larger scales where biofilm spatial patterns are observed (1–100 m), since small-scale biophysical interactions can control spatial organization at larger scales [*Nikora et al*., 1998; *Coco et al*., 2006; *Murray et al*., 2008; *Larsen and Harvey*, 2010; *Meire et al*., 2014]. Long-term studies will also provide clues for how particle fluxes and interactions vary across seasonal cycles and episodic events that, for example, could result in nonstationarity of the power-law RTDs identified in our study. Lastly, new process models (e.g., stochastic transport) must be developed to accommodate the hierarchy of scales and processes that influence fluvial ecosystem function [*Nikora*, 2010; *Boano et al*., 2014; *Marion et al*., 2014]. Such a framework is required to properly relate laboratory observations (e.g., mm-scale flow-biofilm interactions) to those for the entire fluvial network (e.g., time history of high flow events). These models will provide a tool to explore scale interdependencies that currently cannot be observed, either experimentally or in the field, and predict how longer-term shifts in land use and climate may alter overall fine particle fluxes in streams [*Battin et al*., 2009; *Quinton et al*., 2010; *Tank et al*., 2010; *Pizzuto et al*., 2014].

5. Conclusions

These experiments show that particles are retained in benthic biofilms across a wide range of timescales (seconds to months). Application of a stochastic mobile-immobile model indicates that fine particle retention probabilities in biofilm-covered streambeds follow a heavy-tailed power-law distribution ($\varphi(t) \sim t^{-(1+\beta)},\ 0 < \beta < 1$). Particle retention, parameterized by β, was enhanced by increases in mean biofilm height, biofilm roughness, and streambed coverage. These correlations suggest that retention is controlled by biofilm structure, and that biofilm structural parameters should be incorporated into upscaled models for fine particle retention in streams and rivers. However, no biofilm structural parameters were correlated with fine particle deposition rate. Definitive conclusions of deposition-structure interactions require improved experimental capability that can resolve discrete particle deposition and resuspension events at the scales of turbulence. Our results direct future experimental efforts to finer scales (1–100 μm) to elucidate the relative importance of microscale physical structure, surface chemistry, and biofilm matrix composition to overall particle deposition and retention. They also call for a multiscale approach to modeling fluvial transport of fine particles, since the process interactions influencing particle retention may be active at different spatial and temporal scales from those influencing deposition.

Acknowledgments
The authors thank Michael Wagner (KIT, Karlsruhe) for his initial help with OCT. Hannes Hager, Kyle Boodoo, and Gertraud Steniczka (WasserCluster Lunz, Austria) are acknowledged for helping with the experiments and particle analysis. This study was funded by a Marie Curie Intra-European Fellowship to WRH (FP7-PEOPLE-2011-IEF-302297) and an Austrian Science Fund grant to T.J.B. (START Y420-B17). K.R.R. was supported by a CUAHSI Pathfinder fellowship and U.S. NSF Graduate Research Fellowship. J.D.D. was supported by a Fulbright-Spain fellowship. The modeling effort was supported by U.S. NSF grants EAR-1215898 and EAR-1344280 to AIP. Supporting data are provided at doi:10.6084/m9.figshare.4252193. We thank three anonymous reviewers and the associate editor for their extensive comments, which helped us greatly to improve the manuscript.

References

Akaike, H. (1974), A new look at the statistical model identification, *IEEE Trans. Autom. Control*, *19*(6), 716–723.
Allan, J. D., and M. M. Castillo (2007), *Stream Ecology: Structure and Function of Running Waters*, 2 ed., Springer, Dordrecht, Netherlands.
Anderson, R. S., and S. P. Anderson (2010), *Geomorphology: The Mechanics and Chemistry of Landscapes*, Cambridge Univ. Press, Cambridge, U. K.

Arnon, S., L. P. Marx, K. E. Searcy, and A. I. Packman (2010), Effects of overlying velocity, particle size, and biofilm growth on stream-subsurface exchange of particles, *Hydrol. Processes*, *24*(1), 108–114.
Aubeneau, A. F., J. D. Drummond, R. Schumer, D. Bolster, J. L. Tank, and A. I. Packman (2015), Effects of benthic and hyporheic reactive transport on breakthrough curves, *Freshwater Sci.*, *34*(1), 301–315.
Aubeneau, A. F., B. Hanrahan, D. Bolster, and J. Tank (2016), Biofilm growth in gravel bed streams controls solute residence time distributions, *J. Geophys. Res. Biogeosci.*, *121*, 1840–1850, doi:10.1002/2016JG003333.
Battin, T. J., and D. Sengschmitt (1999), Linking sediment biofilms, hydrodynamics, and river bed clogging: Evidence from a large river, *Microb. Ecol.*, *37*(3), 185–196.
Battin, T. J., L. A. Kaplan, J. D. Newbold, and C. M. Hansen (2003), Contributions of microbial biofilms to ecosystem processes in stream mesocosms, *Nature*, *426*(6965), 439–442.
Battin, T. J., L. A. Kaplan, S. Findlay, C. S. Hopkinson, E. Marti, A. I. Packman, J. D. Newbold, and F. Sabater (2008), Biophysical controls on organic carbon fluxes in fluvial networks, *Nat. Geosci.*, *1*(2), 95–100.
Battin, T. J., S. Luyssaert, L. A. Kaplan, A. K. Aufdenkampe, A. Richter, and L. J. Tranvik (2009), The boundless carbon cycle, *Nat. Geosci.*, *2*(9), 598–600.
Battin, T. J., K. Besemer, M. M. Bengtsson, A. M. Romani, and A. I. Packmann (2016), The ecology and biogeochemistry of stream biofilms, *Nat. Rev. Microbiol.*, *14*(4), 251–263.
Berkowitz, B., A. Cortis, M. Dentz, and H. Scher (2006), Modeling non-Fickian transport in geological formations as a continuous time random walk, *Rev. Geophys.*, *44*, RG2003, doi:10.1029/2005RG000178.
Besemer, K., G. Singer, I. Hödl, and T. J. Battin (2009), Bacterial community composition of stream biofilms in spatially variable-flow environments, *Appl. Environ. Microbiol.*, *75*(22), 7189–7195.
Biggs, B. J. F. (1995), The contribution of flood disturbance, catchment geology and land use to the habitat template of periphyton in stream ecosystems, *Freshwater Biol.*, *33*(3), 419–438.
Birjiniuk, A., N. Billings, E. Nance, J. Hanes, K. Ribbeck, and P. S. Doyle (2014), Single particle tracking reveals spatial and dynamic organization of the *Escherichia coli* biofilm matrix, *New J. Phys.*, *16*(8), 085014.
Boano, F., A. Packman, A. Cortis, R. Revelli, and L. Ridolfi (2007), A continuous time random walk approach to the stream transport of solutes, *Water Resour. Res.*, *43*, W10425, doi:10.1029/2007WR006062.
Boano, F., J. W. Harvey, A. Marion, A. I. Packman, R. Revelli, L. Ridolfi, and A. Wörman (2014), Hyporheic flow and transport processes: Mechanisms, models, and biogeochemical implications, *Rev. Geophys.*, *52*(4), 603–679.
Bottacin-Busolin, A., G. Singer, M. Zaramella, T. J. Battin, and A. Marion (2009), Effects of streambed morphology and biofilm growth on the transient storage of solutes, *Environ. Sci. Technol.*, *43*(19), 7337–7342.
Boulêtreau, S., F. Garbétian, S. Sauvage, and J.-M. Sánchez-Pérez (2006), Assessing the importance of a self-generated detachment process in river biofilm models, *Freshwater Biol.*, *51*(5), 901–912.
Bouwer, E. J. (1987), Theoretical investigation of particle deposition in biofilm systems, *Water Res.*, *21*(12), 1489–1498.
Coco, G., S. F. Thrush, M. O. Green, and J. E. Hewitt (2006), Feedbacks between bivalve density, flow, and suspended sediment concentration on patch stable states, *Ecology*, *87*(11), 2862–2870.
Cortis, A., and B. Berkowitz (2005), Computing "anomalous" contaminant transport in porous media: The CTRW MATLAB toolbox, *Groundwater*, *43*(6), 947–950.
Costerton, J. W., Z. Lewandowski, D. E. Caldwell, D. R. Korber, and H. M. Lappin-Scott (1995), Microbial Biofilms, *Annu. Rev. Microbiol.*, *49*(1), 711–745.
Cushing, C. E., G. W. Minshall, and J. D. Newbold (1993), Transport dynamics of fine particulate organic matter in two Idaho streams, *Limnol. Oceanogr.*, *38*, 1101–1115.
Cuthbert, M. O., R. Mackay, V. Durand, M. F. Aller, R. B. Greswell, and M. O. Rivett (2010), Impacts of river bed gas on the hydraulic and thermal dynamics of the hyporheic zone, *Adv. Water Resour.*, *33*(11), 1347–1358.
de Hoog, F., J. Knight, and A. Stokes (1982), An improved method for numerical inversion of Laplace transforms, *SIAM J. Sci. Stat. Comput.*, *3*(3), 357–366.
DiCesare, E. A. W., B. R. Hargreaves, and K. L. Jellison (2012), Biofilm roughness determines *Cryptosporidium parvum* retention in environmental biofilms, *Appl. Environ. Microbiol.*, *78*(12), 4187–4193.
Dimock, R., and E. Morgenroth (2006), The influence of particle size on microbial hydrolysis of protein particles in activated sludge, *Water Res.*, *40*(10), 2064–2074.
Drummond, J., A. Aubeneau, and A. Packman (2014a), Stochastic modeling of fine particulate organic carbon dynamics in rivers, *Water Resour. Res.*, *50*, 4341–4356, doi:10.1002/2013WR014665.
Drummond, J., R. J. Davies-Colley, R. Stott, J. P. Sukias, J. W. Nagels, A. Sharp, and A. I. Packman (2014b), Retention and remobilization dynamics of fine particles and microorganisms in pastoral streams, *Water Res.*, *66*, 459–472.
Drury, W. J., P. S. Stewart, and W. G. Characklis (1993a), Transport of 1-μm latex particles in pseudomonas aeruginosa biofilms, *Biotechnol. Bioeng.*, *42*(1), 111–117.
Drury, W. J., W. G. Characklis, and P. S. Stewart (1993b), Interactions of 1 μm latex particles with *Pseudomonas aeruginosa* biofilms, *Water Res.*, *27*(7), 1119–1126.
Fellows, C., H. M. Valett, C. N. Dahm, P. J. Mulholland, and S. A. Thomas (2006), Coupling nutrient uptake and energy flow in headwater streams, *Ecosystems*, *9*(5), 788–804.
Fisher, S. G., and G. E. Likens (1973), Energy flow in Bear Brook, New Hampshire: An integrative approach to stream ecosystem metabolism, *Ecol. Monogr.*, *43*(4), 421–439.
Flemming, H.-C., and J. Wingender (2010), The biofilm matrix, *Nat. Rev. Microbiol.*, *8*(9), 623–633.
Flemming, H.-C., J. Wingender, U. Szewzyk, P. Steinberg, S. A. Rice, and S. Kjelleberg (2016), Biofilms: An emergent form of bacterial life, *Nat. Rev. Microbiol.*, *14*(9), 563–575.
Flood, J., and N. Ashbolt (2000), Virus-sized particles are concentrated and maintained within wastewater wetland biofilms, *Adv. Environ. Res.*, *3*, 403–411.
Gomi, T., R. C. Sidle, and J. S. Richardson (2002), Understanding processes and downstream linkages of headwater systems, *BioScience*, *52*(10), 905–916.
Harvey, J., et al. (2012), Hydrogeomorphology of the hyporheic zone: Stream solute and fine particle interactions with a dynamic streambed, *J. Geophys. Res.*, *117*, G00N11, doi:10.1029/2012JG002043.
Huang, D., E. A. Swanson, C. P. Lin, J. S. Schuman, W. G. Stinson, W. Chang, M. R. Hee, T. Flotte, K. Gregory, and C. A. Puliafito (1991), Optical coherence tomography, *Science*, *254*(5035), 1178.

Hunter, W. R., R. Niederdorfer, A. Gernand, B. Veuger, J. Prommer, M. Mooshammer, W. Wanek, and T. J. Battin (2016), Metabolism of mineral-sorbed organic matter depends upon microbial lifestyle in fluvial ecosystems, *Geophys. Res. Lett.*, *43*, 1582–1588.
Jones, J. B., and P. J. Mulholland (1999), *Streams and Ground Waters*, Academic, San Diego, Calif.
Karwan, D. L., and J. E. Saiers (2012), Hyporheic exchange and streambed filtration of suspended particles, *Water Resour. Res.*, *48*, W01519, doi:10.1029/2011WR011173.
Larned, S. T., V. I. Nikora, and B. J. Biggs (2004), Mass-transfer-limited nitrogen and phosphorus uptake by stream periphyton: A conceptual model and experimental evidence, *Limnol. Oceanogr. Methods*, *49*(6), 1992–2000.
Larned, S. T., A. I. Packman, D. R. Plew, and K. Vopel (2011), Interactions between the mat-forming alga *Didymosphenia geminata* and its hydrodynamic environment, *Limnol. Oceanogr. Methods*, *1*, 4–22.
Larsen, L. G., and J. W. Harvey (2010), How vegetation and sediment transport feedbacks drive landscape change in the everglades and wetlands worldwide, *Am. Nat.*, *176*(3), E66–E79.
Lock, M. A., and D. D. Williams (1981), River epilithon—A light and organic energy transducer, in *Perspectives in Running Water Ecology*, edited by M. A. Lock, pp. 3–40, Springer, New York.
Margolin, G., M. Dentz, and B. Berkowitz (2003), Continuous time random walk and multirate mass transfer modeling of sorption, *Chem. Phys.*, *295*(1), 71–80.
Marion, A., et al. (2014), Aquatic interfaces: A hydrodynamic and ecological perspective, *J. Hydraul. Res.*, *52*(6), 744–758.
McClain, M. E., et al. (2003), Biogeochemical hot spots and hot moments at the interface of terrestrial and aquatic ecosystems, *Ecosystems*, *6*(4), 301–312.
McNair, J. N., and J. D. Newbold (2012), Turbulent particle transport in streams: Can exponential settling be reconciled with fluid mechanics?, *J. Theor. Biol.*, *300*, 62–80.
Meire, D. W. S. A., J. M. Kondziolka, and H. M. Nepf (2014), Interaction between neighboring vegetation patches: Impact on flow and deposition, *Water Resour. Res.*, *50*, 3809–3825, doi:10.1002/2013WR015070.
Montgomery, D. C., and G. C. Runger (2010), *Applied Statistics and Probability for Engineers*, John Wiley, Hoboken, N. J.
Morales, C. F. L., M. Strathmann, and H.-C. Flemming (2007), Influence of biofilms on the movement of colloids in porous media: Implications for colloid facilitated transport in subsurface environments, *Water Res.*, *41*(10), 2059–2068.
Morgenroth, E., and K. Milferstedt (2009), Biofilm engineering: Linking biofilm development at different length and time scales, *Rev. Environ. Sci. Biotechnol.*, *8*(3), 203–208.
Murray, A. B., M. A. F. Knaapen, M. Tal, and M. L. Kirwan (2008), Biomorphodynamics: Physical-biological feedbacks that shape landscapes, *Water Resour. Res.*, *44*, W11301, doi:10.1029/2007WR006410.
Newbold, J. D., T. L. Bott, L. A. Kaplan, B. W. Sweeney, and R. L. Vannote (1997), Organic matter dynamics in White Clay Creek, Pennsylvania, USA, *J. N. Am. Benthol. Soc.*, *16*(1), 46–50.
Newbold, J. D., S. A. Thomas, G. W. Minshall, C. E. Cushing, and T. Georgian (2005), Deposition, benthic residence, and resuspension of fine organic particles in a mountain stream, *Limnol. Oceanogr. Methods*, *50*(5), 1571–1580.
Nikora, V. I. (2010), Hydrodynamics of aquatic ecosystems: An interface between ecology, biomechanics and environmental fluid mechanics, *River Res. Appl.*, *26*(4), 367–384.
Nikora, V. I., A. M. Suren, S. L. Brown, and B. J. Biggs (1998), The effects of the moss Fissidens rigidulus (Fissidentaceae: Musci) on near-bed flow structure in an experimental cobble bed flume, *Limnol. Oceanogr.*, *43*(6), 1321–1331.
Nikora, V. I., D. G. Goring, and B. J. F. Biggs (2002), Some observations of the effects of micro-organisms growing on the bed of an open channel on the turbulence properties, *J. Fluid Mech.*, *450*, 317–341.
Niño, Y., F. Lopez, and M. Garcia (2003), Threshold for particle entrainment into suspension, *Sedimentology*, *50*(2), 247–263.
Ninto, Y., and M. H. Garcia (1996), Experiments on particle-turbulence interactions in the near-wall region of an open channel flow: Implications for sediment transport, *J. Fluid Mech.*, *326*, 285–319.
Okabe, S., T. Yasuda, and Y. Watanabe (1997), Uptake and release of inert fluorescence particles by mixed population biofilms, *Biotechnol. Bioeng.*, *53*(5), 459–469.
Okabe, S., H. Kuroda, and Y. Watanabe (1998), Significance of biofilm structure on transport of inert particulates into biofilms, *Water Sci. Technol.*, *38*(8), 163–170.
Paul, M. J., and R. O. Hall Jr. (2002), Particle transport and transient storage along a stream-size gradient in the Hubbard Brook Experimental Forest, *J. N. Am. Benthol. Soc.*, *21*(2), 195–205.
Pizzuto, J., et al. (2014), Characteristic length scales and time-averaged transport velocities of suspended sediment in the mid-Atlantic Region, U.S.A., *Water Resour. Res.*, *50*, 790–805, doi:10.1002/2013WR014485.
Power, M. E., and A. J. Stewart (1987), Disturbance and recovery of an algal assemblage following flooding in an Oklahoma Stream, *Am. Midland Nat.*, *117*(2), 333–345.
Quinton, J. N., G. Govers, K. Van Oost, and R. D. Bardgett (2010), The impact of agricultural soil erosion on biogeochemical cycling, *Nat. Geosci.*, *3*(5), 311–314.
R Development Core Team (2009), *R: A Language and Environment for Statistical Computing*, R Found. for Stat. Comput., Vienna, Austria.
Richardson, D. C., J. D. Newbold, A. K. Aufdenkampe, P. G. Taylor, and L. A. Kaplan (2013), Measuring heterotrophic respiration rates of suspended particulate organic carbon from stream ecosystems, *Limnol. Oceanogr. Methods*, *11*, 247–261.
Rouse, H. (1939), Experiments on the mechanics of sediment suspension, in Proceedings of the Fifth International Congress for Applied Mechanics, pp. 550–554, John Wiley, New York.
Schindelin, J., et al. (2012), Fiji: An open-source platform for biological-image analysis, *Nat. Methods*, *9*(7), 676–682.
Schneider, C. A., W. S. Rasband, and K. W. Eliceiri (2012), NIH image to ImageJ: 25 years of image analysis, *Nat. Methods*, *9*(7), 671–675.
Schumer, R., D. A. Benson, M. M. Meerschaert, and B. Baeumer (2003), Fractal mobile/immobile solute transport, *Water Resour. Res.*, *39*(10), 1296, doi:10.1029/2003WR002141.
Searcy, K. E., A. I. Packman, E. R. Atwill, and T. Harter (2006), Capture and retention of Cryptosporidium parvum oocysts by *Pseudomonas aeruginosa* biofilms, *Appl. Environ. Microbiol.*, *72*(9), 6242–6247.
Soldati, A., and C. Marchioli (2009), Physics and modelling of turbulent particle deposition and entrainment: Review of a systematic study, *Int. J. Multiphase Flow*, *35*(9), 827–839.
Stonedahl, S. H., J. W. Harvey, J. Detty, A. Aubeneau, and A. I. Packman (2012), Physical controls and predictability of stream hyporheic flow evaluated with a multiscale model, *Water Resour. Res.*, *48*, W10513, doi:10.1029/2011WR011582.
Stoodley, P., Z. Lewandowski, J. D. Boyle, and H. M. Lappin-Scott (1999), Structural deformation of bacterial biofilms caused by short-term fluctuations in fluid shear: An in situ investigation of biofilm rheology, *Biotechnol. Bioeng.*, *65*(1), 83–92.

Stoodley, P., R. Cargo, C. Rupp, S. Wilson, and I. Klapper (2002), Biofilm material properties as related to shear-induced deformation and detachment phenomena, *J. Ind. Microbiol. Biotechnol.*, *29*(6), 361–367.

Sutherland, I. W. (2001), The biofilm matrix—An immobilized but dynamic microbial environment, *Trends Microbiol.*, *9*(5), 222–227.

Taherzadeh, D., C. Picioreanu, and H. Horn (2012), Mass transfer enhancement in moving biofilm structures, *Biophys. J.*, *102*(7), 1483–1492.

Tank, J. L., E. J. Rosi-Marshall, N. A. Griffiths, S. A. Entrekin, and M. L. Stephen (2010), A review of allochthonous organic matter dynamics and metabolism in streams, *J. N. Am. Benthol. Soc.*, *29*(1), 118–146.

Thomas, S. A., J. D. Newbold, M. T. Monaghan, G. W. Minshall, T. Georgian, and C. E. Cushing (2001), The influence of particle size on seston deposition in streams, *Limnol. Oceanogr.*, *46*(6), 1415–1424.

Vignaga, E., D. M. Sloan, X. Luo, H. Haynes, V. R. Phoenix, and W. T. Sloan (2013), Erosion of biofilm-bound fluvial sediments, *Nat. Geosci.*, *6*(9), 770–774.

Wagner, M., D. Taherzadeh, C. Haisch, and H. Horn (2010), Investigation of the mesoscale structure and volumetric features of biofilms using optical coherence tomography, *Biotechnol. Bioeng.*, *107*(5), 844–853.

Weiss, N., T. G. van Leeuwen, and J. Kalkman (2013), Localized measurement of longitudinal and transverse flow velocities in colloidal suspensions using optical coherence tomography, *Phys. Rev. E*, *88*(4), 042312.

Xi, C., D. Marks, S. Schlachter, W. Luo, and S. A. Boppart (2006), High-resolution three-dimensional imaging of biofilm development using optical coherence tomography, *J. Biomed. Opt.*, *11*(3), 034001–034006.

Xu, L.-C., V. Vadillo-Rodriguez, and B. E. Logan (2005), Residence time, loading force, pH, and ionic strength affect adhesion forces between colloids and biopolymer-coated surfaces, *Langmuir*, *21*(16), 7491–7500.